https://doi.org/10.22320/s0718221x/2026.08
ARTÍCULO

Comparative evaluation of three-way mortise-and-tenon joint designs considering mechanical strength and machinability

Yuqing Yang[1] https://orcid.org/0009-0000-7208-0087
Zhongyuan Zhao[1] https://orcid.org/0000-0002-8787-8267
Wen-gang Hu[1] https://orcid.org/0000-0001-8077-6324♠

[1]Nanjing Forestry University. College of Furnishings and Industrial Design. Nanjing. China.

♠Corresponding author: hwg@njfu.edu.cn

Abstract:
It is still a challenge to manufacture traditional three-way Zongjiao mortise-and-tenon joints using modern CNC-based machines. This study aimed to improve the structure of the Zongjiao mortise-and-tenon joint, a commonly used three-way corner joint in wood furniture, to better align with modern manufacturing practices. First, four improved mortise-and-tenon joint types were designed, and their appearances were evaluated. Secondly, mechanical tests and numerical analyses were conducted to compare the four improved types and two previous types using bending strength and load difference ratio (DR) between the two horizontal members of the joint. Subsequently, the machinability of all types of joints was evaluated through processing time (PT), cutting force (CF), and number of effective programs (NEP). The results showed that the maximum bending strength of the Zongjiao M-T joint was observed in Type D, and the load DR between the two horizontal members was 13,79. The improved Type D has the lowest milling CF of 182 N and the minimum PT of 32 minutes with the least NEP. Through a comprehensive analysis of all the above indices evaluated, it was found that the improved Type D of Zongjiao mortise-and-tenon joint was superior to others, considering appearance, mechanical strength, and machinability. This study provided a paradigm for optimizing wood furniture joints, which can also be applied to other wood products.

Keywords: Bending strength, furniture machinability, wood joint, wood machine.

Received: 14.05.2025
Accepted: 09.03.2026

Introduction

Mortise-and-tenon (M-T) joints are widely used in wood constructions and wood products, such as furniture, doors, windows, and stairs. Many researchers tried to optimize M-T joints to get high strengths in terms of size (Kiliç *et al*. 2018, Záborsky *et al*. 2017a, Hu and Chen 2021), wood species (Záborsky *et al*. 2017a, Zhu and Niu 2022, Luo *et al*. 2023), and tenon fit (Záborsky *et al*. 2017b, Liu *et al*. 2024) and glue type (Záborsky *et al*. 2017a, Zou *et al*. 2024a,b, Lin *et al*. 2023, Bai *et al*. 2024).

Zongjiao M-T joint, a three-way corner joint, is a traditional furniture connecting method (Figure 1), commonly used to construct the tabletop and the legs of tables (Tang *et al*. 2022, Zhao *et al*. 2021, Qi *et al*. 2023). The connections between different components of Zongjiao M-T joints generate structural lines as prominent appearance features, which is an attractive aspect of furniture (Chen and Xu 2024, Zhou *et al*. 2024a, Zhou *et al*. 2024b, Lu *et al*. 2024). However, it is composed of three members vertically connected in three directions, making its internal structure relatively complex compared to other M-T joints. The traditional processing method of the Zongjiao M-T joint was mainly manufactured by hand with low efficiency. Meanwhile, modern automated processing methods, such as five-axis Computer Numerical Control (CNC) machine tools and tenon milling machines, have high costs and inflexibility (Xiong *et al*. 2024, Wang and Yan 2024). Processing a rectangle mortise is tough work for modern machines. This dilemma needs to be solved to make the Zongjiao M-T joint alive in modern wood products.

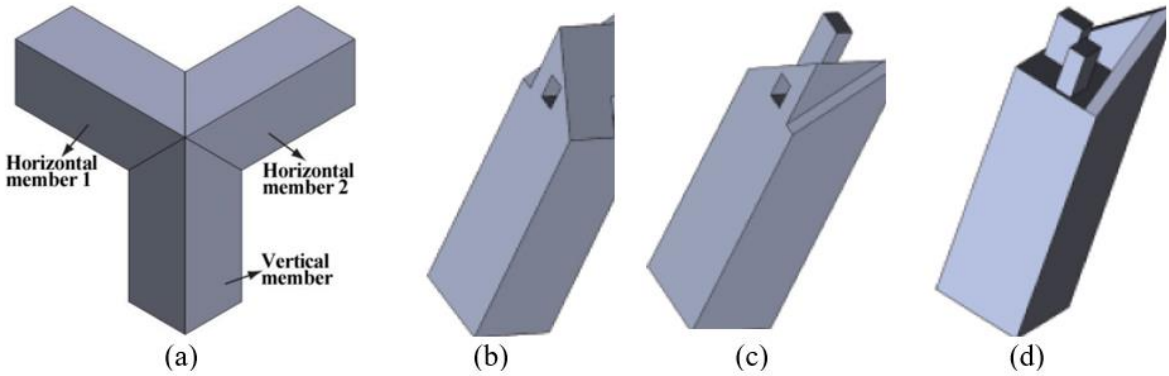

Figure 1: Construction of a traditional Zongjiao M-T joints: (a) assembly, (b) horizontal member 1, (c) horizontal member 2, and (d) vertical member.

Upon the improvement of the Zongjiao M-T joint, some researchers had made attempts. Among these studies, Zhao *et al*. (2021) proposed a new improved type of Zongjiao M-T joint considering its processing efficiency, bending strength, and appearance. The results showed that the proposed method not only retained the appearance of the Zongjiao M-T joint but also increased the bending strength by 20 %. However, the processing time increased by 15 %. Tang *et al*. (2019) compared the strength and processing time of hand-made Zongjiao M-T joints and CNC-made improved joints. The results showed that both the strength and processing time of the CNC-made Zongjiao M-T joint were improved over those of the hand-made Zongjiao M-T joint. These studies proposed new methods of manufacturing Zongjiao M-T joints to suit the modern manufacturing processing machines. However, the Zongjiao M-T joint still has potential to be improved by considering the processing parameters and strength.

With technological advancements, the processing method of M-T joints has evolved from manual to automated processing. Some researchers have used computer-aided manufacturing to improve the design and analysis of M-T structures (Uysal *et al*. 2019, Tang *et al*. 2019, Tang *et al*. 2022). Computer-aided engineering (CAE) is widely used to design, improve, and

analyze M-T structures (Hu and Chen 2021, Kasal *et al*. 2016, Miao *et al*. 2022), particularly the finite element method, which has been widely used to simulate the mechanical strength of M-T structures. Concerning the finite element method (FEM) used in wood furniture, previous studies utilized FEM to optimize the entire furniture structures and joints (Prekrat and Smardzewski 2010, Smardzewski 2008, Zheng *et al*. 2024). In these studies, the wood was regarded as an orthotropic material, and M-T joints were rigid or semi-rigid contacts. These studies proved that it can be used as a validated method in comparative analysis.

Integrating computer-aided technology and automated manufacturing equipment with M-T joints helped optimize structural performance, improve production efficiency, and preserve excellent traditional culture. This study aimed to propose improved methods of manufacturing the Zongjiao M-T joints to be compatible with modern processing methods. Specifically, four new types of Zongjiao M-T joints were designed and compared with the existing two types reported in published results in terms of machinability and strength based on experimental and numerical methods. The optimal type was obtained by comprehensively analyzing all evaluated indices.

Materials and methods

Materials

The beech (*Fagus orientalis* Lipsky) wood is commonly used in manufacturing wood products, especially in China and Europe, due to its adequate strength and delicate grain. In this study, beech wood lumbers were bought from a local commercial wood supplier (Nanjing, China), imported from Europe, and stored in the laboratory for more than 12 months to reach air-dry condition before manufacturing samples. The moisture content and density of beech wood were 12 % and 700 kg/m^3.

Specimen preparations and appearance evaluation

Figure 2 shows the dimensions (unit: mm) of all types of Zongjiao M-T joints A, B, C, D, E, and F, respectively. Among these types, A, B, C, and D were proposed in this study. Types E and F were designed by previous researchers, Tang *et al*. (2022) and Xue (2013), respectively. The outline dimensions of all specimens are identical, measured at 40 × 40 × 150 mm, but the dimensions of the mortise and tenon are various. All samples were constructed by three members and assembled without glue. One aim of this study was to keep the appearance of the traditional Zongjiao M-T joint as much as possible. Therefore, the appearances of all proposed types were also set as an index to evaluate all types of joints in terms of external structural lines compared with the traditional Zongjiao M-T joints.

The score of each joint's appearance was shown in Table 1. All types of joints nearly retain the appearance of the traditional joint, except Type A. The improved Zongjiao M-T joint Type A came from a traditional Zongjiao M-T joint structure known as a double tenon Zongjiao

M-T joint. This structure had two tenons, one long and one short, fixed at the bottom of the vertical specimen. The two tenons engaged with the two mortises on the horizontal component, thereby facilitating the connection of the three individual members. The horizontal specimens were connected using cube-shaped tenons and mortises, with the structural line exposed at the top of one of the horizontal specimens. In the improved Type B, the internal shape of the Zongjiao M-T joint resembled ancient Chinese city walls (Deng *et al*. 2024a,b).

The horizontal and vertical specimens were tightly connected by serrated tenons and mortises. The characteristic of the improved Type C had a corresponding circular mortise on both sides of the vertical specimen and at the bottom of the horizontal specimen. The vertical and horizontal specimens were connected by a total of four circular wood tenons, bought from a commercial wood shop, in two directions, with the lengths of the circular tenons staggered to maximize the internal space of the specimen. In improved Type D, each specimen had the same shape with two slopes, and they were connected by wood domino tenons bought from a commercial wood shop.

(a)

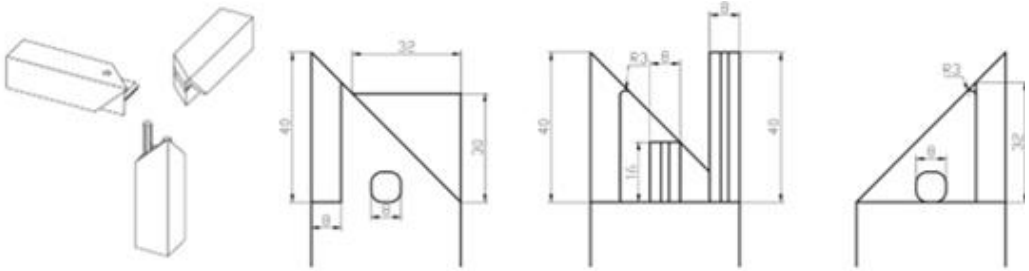

(b)

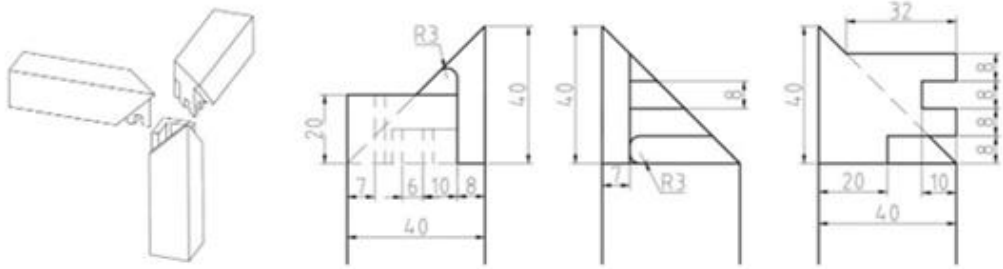

(c)

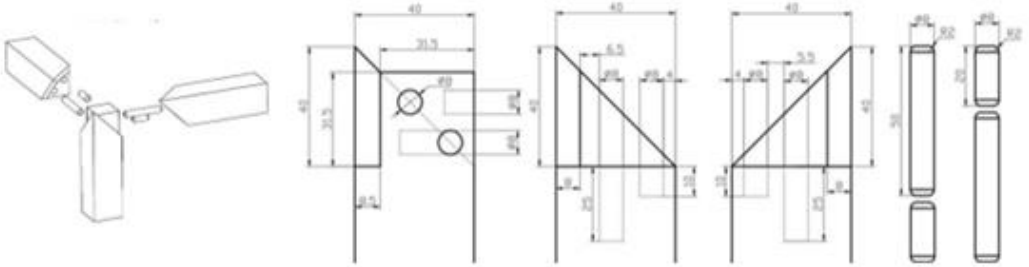

(d)

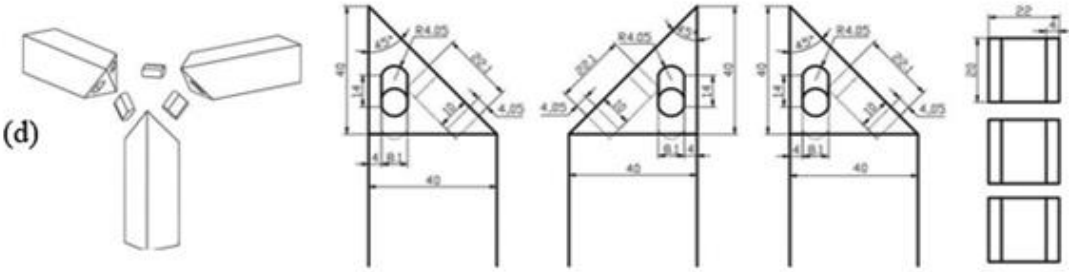

(e)

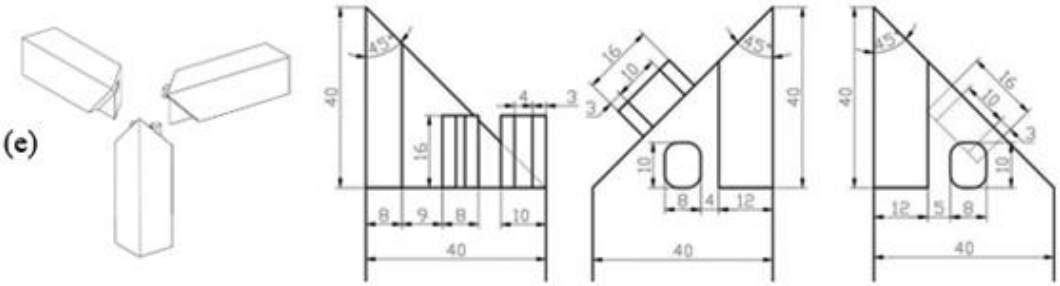

(f)

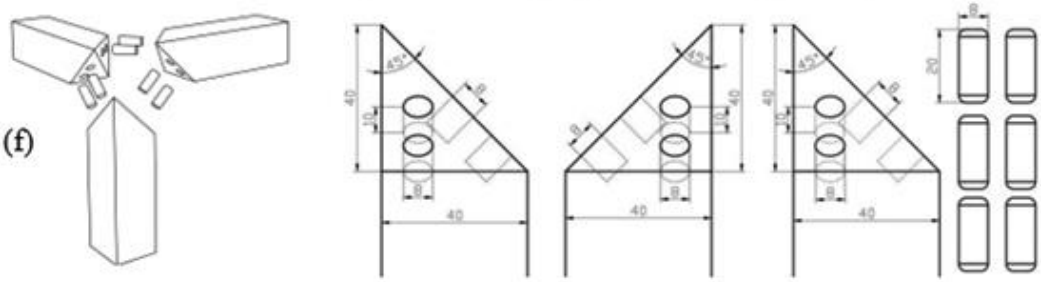

Figure 2: Dimensions (unit: mm) of specimens: (a) Type A, (b) Type B, (c) Type C, (d) Type D, (e) Type E, and (f) Type F.

Table 1: Scoring the appearance of joints compared with the traditional joint.

Type	A	B	C	D	E	F
Score	5	6	6	6	6	6

Experimental procedure

Bending strength test

Figure 3a illustrates the device used to measure the bending strength of improved Zongjiao M-T joint types using a universal mechanical testing machine (AGS-X, SHAMDZU, Japan). The bottom of the vertical component was fixed, and a vertical downward displacement of 5mm/min was applied at a distance of 140 mm from the end face of the horizontal member. Because the two horizontal members can't be tested synchronously due to a lack of clamps, only one side can be evaluated at a time. For Types A and B, two sides were measured, respectively, because two horizontal members were asymmetric. In terms of Types C and D, only one side was measured since two sides were symmetric. The maximum bending strength and load displacement curve were then recorded. There were 40 samples tested with 10 replications for each improved type.

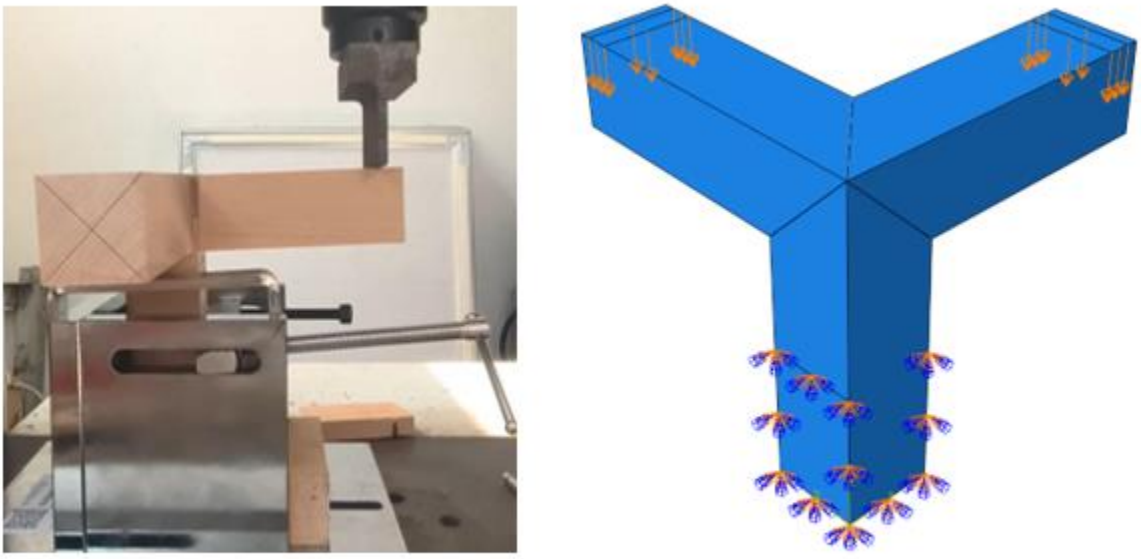

(a) (b)

Figure 3: Setup for measuring the bending strength of Zongjiao M-T joints: (a) mechanical tests, and (b) numerical simulation.

Strength simulation using CAE

To compensate for the deficiencies of experimental tests, Figure 3b shows the finite element model of improved Zongjiao M-T joint types established using ABAQUS (2024, Dassault Systèmes, USA) to evaluate bending strengths at two horizontal members. The modeling methods were referred to our previous study (Hu and Chen 2021), which has been proven to be viable for simulating the strength of M-T joints. The difference ratio (DR) of bending strengths at two horizontal members was calculated by Equation 1 to evaluate if two horizontal members were in equilibrium.

$$DR = \frac{BLR_h - BLR_l}{BLR_h} \quad (1)$$

where BLR_h and BLR_l mean two sides of the Zongjiao M-T joint with high and low bending strengths at two horizontal members, respectively.

The specific modeling method imposes displacement in the dividing line area on the upper surface of the horizontal specimen to simulate the load process. These areas were located 5 mm from the end of the horizontal specimens and have dimensions of 10 × 100 mm. The beech wood was regarded as an orthotropic material by inputting its elastic constants (Hu and Chen 2021). For contact behaviors of the Zongjiao M-T joint, the contact attributes include normal and axial behavior. The tangential friction formula was defined as “penalty”, and the friction coefficient was set to 0,54. Universal contact or face-to-face contact was established. In the interaction module, a grounding spring was added at the end of the specimen, with a small spring stiffness, to provide constraints to the horizontal members in the initial analysis step.

Machinability evaluation

The machinability of all proposed types was evaluated based on cutting force (CF), number of effective programs (NEP), and processing time (PT). The number of effective programs is

a parameter to evaluate the complexity of the G-code input to CNC, which is equal to the total program minus duplicate programs. Process time was obtained based on real manufacturing, while cutting force and number of effective programs were obtained by the virtual processing simulation.

Figure 4 shows a representative processing path of Type A of the Zongjiao M-T joint based on the computer-aided manufacturing software, MasterCAM (2024, CNC Software Inc., USA). The improved Zongjiao M-T joint type models were input into the MasterCAM platform for machining simulation and programming using a virtual 2,5-axis CNC equipment. MasterCam was utilized for cutter path planning and programming. Pre-processing of the machining simulation involved setting machining planes, selecting program types, and configuring machining parameters.

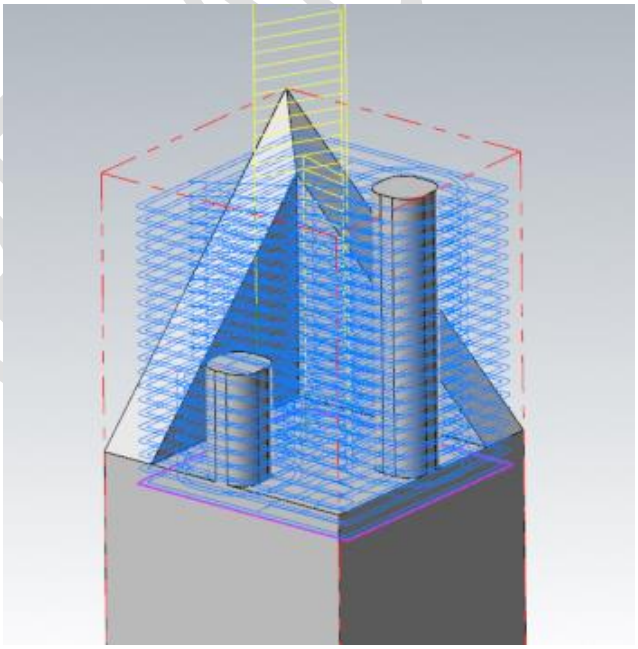

Figure 4: Representative processing path of simulating manufacturing Zongjiao M-T joint of Type A (The red line represents the blank of the wood sample. The line in purple means the boundary of processing. Blue and yellow lines indicate the processing path and the path of removing the drill.)

Manufacturing models of all types of joints were performed in MasterCam. The cutting force and number of effective programs were analyzed by Vericut (7.0, CGTECH, USA). The primary procedure was to input the model of improved Zongjiao M-T joint types into the CAM platform for machining simulation and programming using 2,5-axis CNC equipment. The machine tool was flat end mill with a diameter of 6 mm, and the feed rate was 100 m/min. Finally, all samples were machined using a 2,5-axis CNC machine milling cutter using the programs mentioned above. Processing time was calculated by summing up the processing time of all three members of each type. After completing the improved Zongjiao M-T joint type machining strategy and NC program development, a comparative analysis was conducted on the number of machining programs used for each member, hereinafter referred to as "program quantity". The total number of programs and the number of duplicate programs for each type were counted separately. The number of effective machining programs is equal to the total number of programs minus duplicate programs. Furthermore, the score of each type of joint was obtained based on the rule that the lower the NEP value, the higher the score. For processing time (PT), the shorter the PT, the higher the score. The higher the cutting force (CF), the lower the score.

Strategy of comprehensive comparison

All six types of joints were evaluated based on the following 6 indices: appearance, bending strength, DR, NEP, PT, and CF. Each index has the same weight, and the sum of them is used as the final score to select the optimal type of joint.

Statistical analysis

An analysis of variance (ANOVA) general linear model (GLM) procedure was applied to study the effects of type on the bending strengths of Zongjiao M-T joints. Meanwhile, mean comparisons using the protected least significant difference (LSD) procedure were performed. All statistical analyses were performed at the 5 % significance level using SPSS (version 22.0 IBM, USA). All evaluated variables were normalized and scored to comprehensively compare all types and obtain the optimal type.

Results and discussion

Bending strength of zongjiao M-T joints

Figure 5 shows the load-displacement curves acquired from mechanical testing for each group of four improved Zongjiao M-T joint types. Throughout the loading process, the loading head experienced the reaction force of the horizontal member of the Zongjiao M-T joint. The mechanical behavior of each group in the improved design type of Zongjiao M-T

joint structure can be roughly divided into four stages: the elastic stage, the initial plastic stage, the yield stage, and the failure stage. Initially, in the elastic stage, some improved types showed characteristics of the elastic stage of materials, with the displacement and load following a linear relationship. In the second stage, some types exhibited a curved shape, similar to the initial plastic stage of materials. In the third stage, after reaching the failure load, numerous improved types showed a stepped descent feature. During this stage, the structural stress changed relatively little, but the strain varied significantly. In the final stage, the structure was destroyed and the load rapidly decreased to near zero.

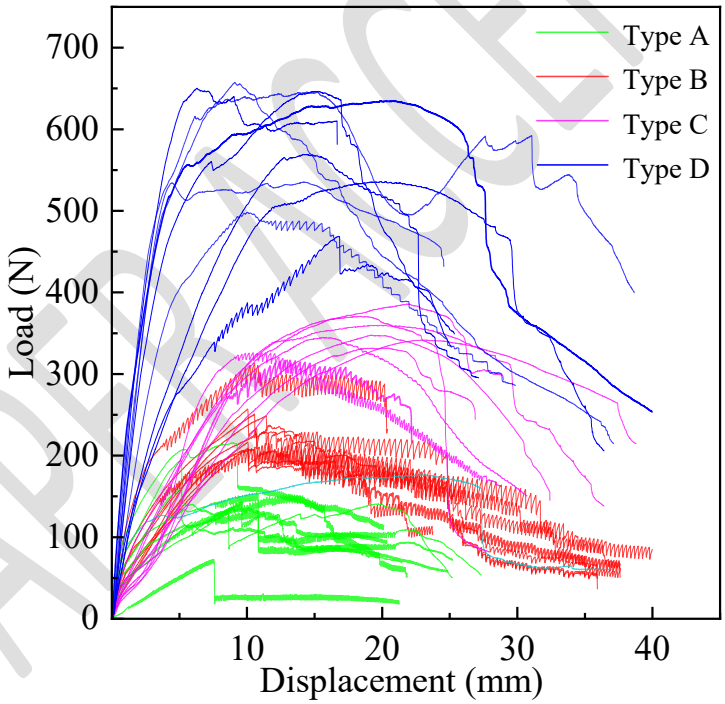

Figure 5: Bending strength-displacement curves of all samples.

Table 2 summarizes the mean values of bending strength (N) of all evaluated joint types and other researchers' types. ANOVA results showed that the M-T joint type had a significant

effect on the bending strength of the joint with a *p*-value of 0,001 and an *F*-value of 53. The mean comparison results show that Type D is significantly stronger than those of other types, which may result from the fact that the geometric dimensions of the domino tenon of the Type D joint are higher than those of other joints. Additionally, two horizontal members of the Type D joint are symmetric, making the Type D joint more stable. Previous studies also reported that the bending strength of the M-T joint increased as the dimensions increased (Kasal *et al*. 2016, Kiliç *et al*. 2018). Compared with Types E, F, and traditional joints reported in previous studies (Tang *et al*. 2022, Xue 2013), the strength of the Type D joint also performed better than them. Furthermore, all types were scored according to the order of bending strength values used for the final comprehensive comparison.

Table 2: Mean comparison of bending strength among the M-T joints.

Type	A	B	C	D	E	F	Traditional
Bending strength (N)	165 (15) D	237(14) C	348(6) B	584(12) A	556	424	527
Displacement (mm)	10,7 (12)	13,2 (13)	19,6 (10)	15,8 (15)	--	--	
Score	1	2	3	6	5	4	

The values in the parentheses are the coefficient of variation (COV) in percentage. The values in the same row not followed by a common letter are significantly different at 5 % significance level.

Strength simulation results of Zongjiao M-T joints

Figure 6 shows the stress distributions of all evaluated types of Zongjiao M-T joints. As load displacement grew, the stress on the internal connecting structure reached its peak and caused

it to separate. For Types C and D, the improved version, they exhibited a trend where the internal tenon was prone to being pulled out with increasing load displacement (Kasal *et al*. 2016). Meanwhile, the mechanical behavior of the two horizontal members was not identical. Due to the different internal structures on the left and right sides of certain improved Zongjiao M-T joint types, they might exhibit varying behaviors when subjected to external forces. If there was a big difference between the horizontal specimens on both sides, it would impact the stability of the overall structure, with the weaker side determining the minimum load-bearing capacity of the structure (Záborsky *et al*. 2017a, Záborsky *et al*. 2017b).

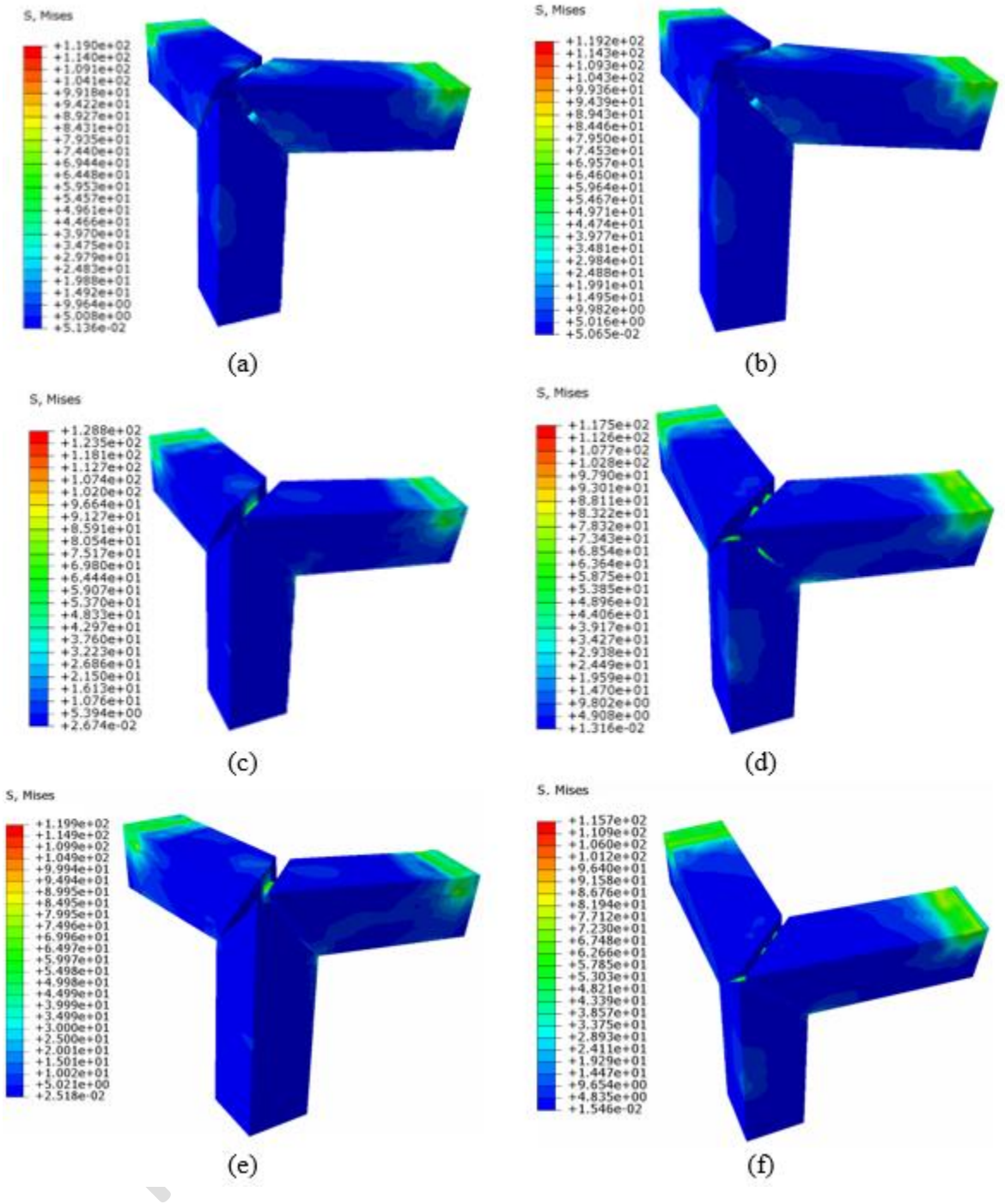

Figure 6: Stress distributions of Zongjiao M-T joints: (a) Type A, (b) Type B, (c) Type C, (d) Type D, (e) Type E, and (f) Type F.

Table 3 shows the difference ratio in bending strength between the two horizontal members based on numerical analysis. The improved Type F joint was the lowest with 7,5 % among

all evaluated joints. These indicate that the mechanical strength of the left horizontal member was 7,5 % higher than that of the right side. However, its maximum bending strength was lower than that of the Type D joint (Table 2). The diameter of the wood dowel used in Type F might influence the bending strength of Type E, as well as the cross-section of members. Furthermore, the score of each type is assigned according to the DR, with the rule that a high score is assigned for low DR.

Table 3: Comparison of the difference ratios of the bending strength between two horizontal members.

Type	A	B	C	D	E	F
DR (%)	20,62	11,34	15,33	13,79	13,24	7,50
Score	1	5	2	4	3	6

Machinability evaluation results

Number of effective programs (NEP)

Table 4 summarizes the number of effective programs (NEP) and score of each type of joint. The improved Type C required the highest total number and variety of programs. Improved Type D required a total of 6 programs, with 4 programs that can be reused, resulting in only 2 effective programs needed.

Table 4: Comparison of the program numbers of all evaluated Zongjiao joint types.

Type	A	B	C	D	E	F
Total number of programs	10	7	13	6	9	12
Number of duplicate programs	2	2	4	4	2	8
NEP	8	5	9	2	7	4
Score	2	4	1	6	3	5

Cutting force (CF)

Table 5 shows that the most optimal solution, with the minimum cutting force, was improved Type D, which had a force of 182 N. In contrast, the maximum cutting force value was found in improved Type C, reaching 473 N. The improved joint Type D had the smallest maximum force value, which was 62 % smaller than the improved joint Type C. The force analysis based on Vericut indicated that due to the influence of parameter setting, the total force of the cutter may not accurately reflect the actual force value of the tool when cutting wood under real conditions. When the parameters of the machine tool, system, tool material, feed rate, etc., remain consistent, the force analysis serves as a standard for evaluating the improved Zongjiao M-T joint type structure (Xiong *et al*. 2024). The score of each joint type was obtained by complying with the rule that a high cutting force brought a low score. Excessive force on the cutting tool during the machining process resulted in tool breakage, posing a risk of injury to personnel (Jiang *et al*. 2022, Yu *et al*. 2023).

Table 5: Comparison of the maximum cutting force of all improved Zongjiao joint types.

Type	A	B	C	D	E	F
Cutting force（N）	270	208	473	182	438	289
Score	4	5	1	6	2	3

Processing time (PT)

Figure 7 shows photos of all machined members of each type using the same 2,5-axis CNC machine milling cutter and processing parameters. Here, the processing time represents the sum of time processing all three members of each type.

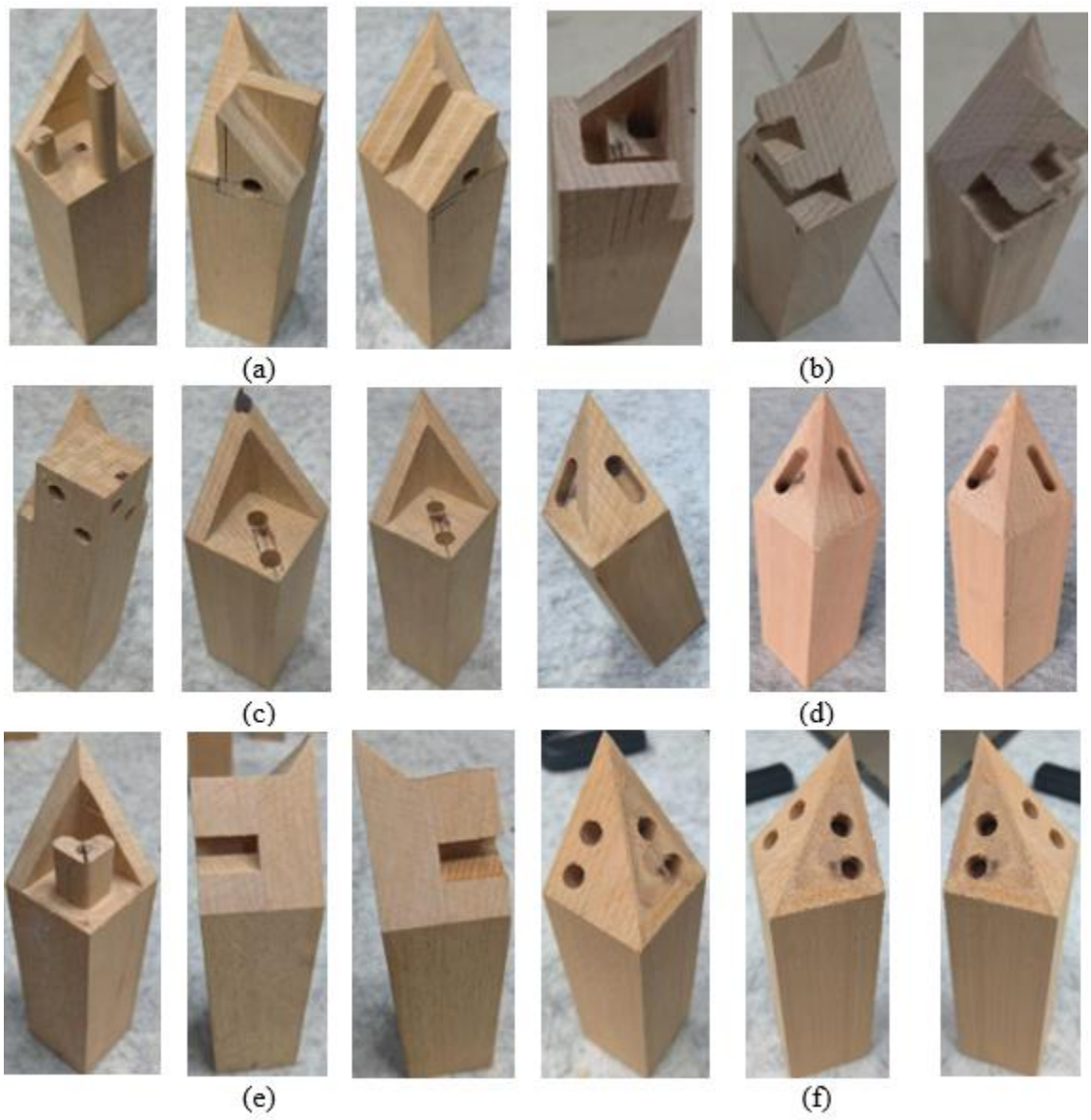

Figure 7: Photos of all processed samples: (a) Type A, (b) Type B, (c) Type C, (d) Type D, (e) Type E, and (f) Type F.

Table 6 shows that the longest PT is the improved joint Type C, which takes 71 minutes. The shortest processing time was the improved joint Type D, which takes only 32 minutes. Improved Type D had reduced the PT by 55 % compared with improved Type C.

Table 6: Comparison of the processing time of all types of improved Zongjiao joints.

Type	A	B	C	D	E	F
Processing time (min)	59	52	71	32	48,5	46
Score	2	3	1	6	4	5

Comprehensive comparisons and analysis

Figure 8 summarizes all the indices for all evaluated types of Zongjiao M-T joints in terms of the scores using a radar chart. The comparison includes mechanical performance, machinability, and the appearance of the joints when the members are assembled (Figure 2), which reflects the visual characteristics of the joint structure. Considering all aspects, it can be concluded that Type D performed better than the others, with the highest score. Meanwhile, furniture manufacturers can select the most suitable joint type according to their production requirements.

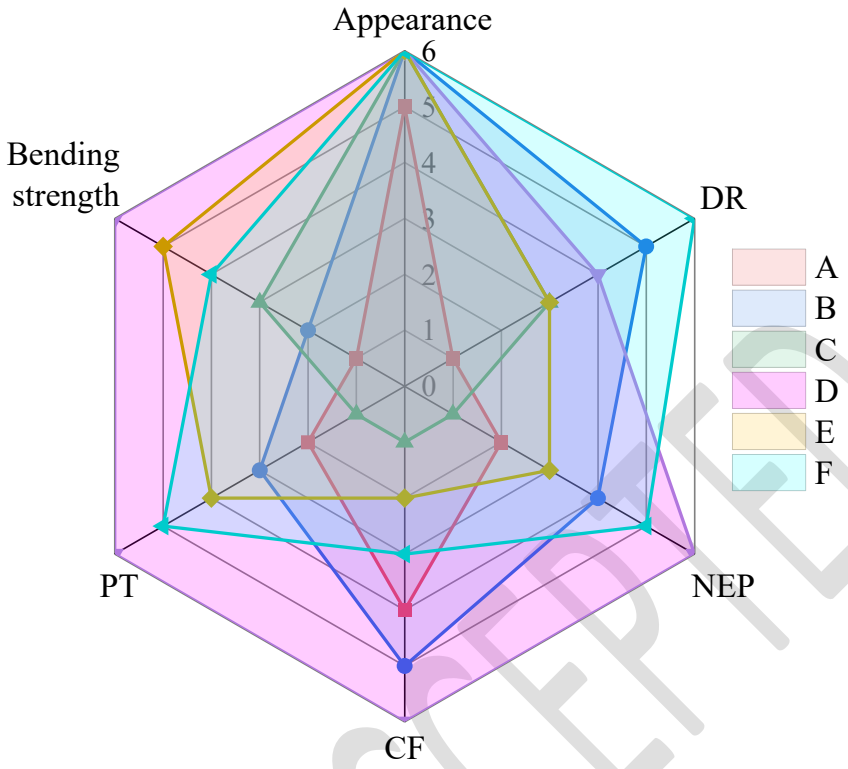

Figure 8: Radar chart of all evaluated types considering all indexes.

Conclusions

In this study, the traditional three-way furniture joint, Zongjiao mortise-and-tenon (M-T) joint, used in wood frame furniture, was investigated to suit the modern manufacturing mode using experimental tests and simulation methods, including computer-aided engineering (CAE), and computer-aided manufacturing (CAM) methods. The following conclusions can be drawn:

1) The proposed three-way M-T joint Type D showed the best overall performance among the evaluated configurations, considering bending strength, the difference ratio (DR)

between horizontal members, cutting force (CF), processing time (PT), and the number of effective programs (NEP).

2) The method of incorporating CAD, CAM, and CAE in optimizing the M-T joint is viable and effective, which can reduce the cost of engineers and designers.
3) It is suggested that using modular connecting elements, such as dowels and domino tenons, is beneficial to make traditional joints to adjust to the modern manufacturing machine.
4) This study presents a paradigm for optimizing wood M-T joints using experimental and simulation methods, which can also be applied to other wood products.

Authorship contributions

Y. Y.: Software, formal analysis, validation, writing-original draft. Z. Z.: Data curation, formal analysis, validation, writing - original draft, writing - review & editing. W. H.: Conceptualization, resources, formal analysis, methodology, writing - original draft, project administration, writing - review & editing.

Acknowledgements

This work is mainly supported by the National Natural Science Foundation of China (32201488), and partially supported by the National Natural Science Foundation of China (32271785).

Conflicts of interest

The authors declare there are no conflicts of interest for each author.

References:

Bai, J.; Guan, H.; Li, Y.; Jiang, S. 2024. Synthesis of phase change microcapsules based dispersants for waterborne coatings and their effects on paint film properties. *Journal of Dispersion Science and Technology* 45(3): 491-502. https://doi.org/10.1080/01932691.2022.2158852

Chen, Y.; Xu, Z. 2024. Research on the evaluation model for the tactile feel of custom wardrobe furniture finishes. *BioResources* 19(3): 5262-5287. https://doi.org/10.15376/biores.19.3.5262-5287

Deng, J.; Ding, T.; Yan, X. 2024a. Optimization of preparation process for chitosan-coated pomelo peel flavonoid microcapsules and its effect on waterborne paint film properties. *Coatings* 14. e1003. https://doi.org/10.3390/coatings14081003

Deng, J.; Ding, T.; Yan, X. 2024b. Effect of two pomelo peel flavonoid microcapsules on the performance of waterborne coatings on the surface of poplar boards. *Coatings* 14. e937. https://doi.org/10.3390/coatings14080937

Hu, W.G.; Chen, B.R. 2021. A methodology for optimizing tenon geometry dimensions of mortise-and-tenon joint wood products. *Forests* 12. e478. https://doi.org/10.3390/f12040478

Jiang, S.; Buck, D.; Tang, Q.; Guan, J.; Wu, Z.; Guo, X.; Zhu, Z.; Wang, X. 2022. Cutting force and surface roughness during straight-tooth milling of walnut wood. *Forests* 13. e2126. https://doi.org/10.3390/f13122126

Kasal, A.; Smardzewski, J.; Kuşkun, T.; Erdil, Y. 2016. Numerical analyses of various sizes of mortise and tenon furniture joints. *BioResources* 11(3): 6836-6853. https://doi.org/10.15376/biores.11.3.6836-6853

Kiliç, H.; Kasal, A.; Kuşkun, T.; Acar, M.; Erdil, Y.Z. 2018. Effect of tenon size on static front to back loading performance of wooden chairs in comparison with acceptable design loads. *BioResources* 13(1): 256-271. https://doi.org/10.15376/biores.13.1.256-271

Luo, Z.; Xu, W.; Wu, S. 2023. Performances of green velvet material (PLON) used in upholstered furniture. *BioResources* 18(3): 5108-5119. https://doi.org/10.15376/biores.18.3.5108-5119

Liu, W.; Zhu, L.; Varodi, A.M.; Liu, X.; Lv, J. 2024. The effect of wet and dry cycles on the strength and the surface characteristics of coromandel lacquer coatings. *Forests* 15. e770. https://doi.org/10.3390/f15050770

Lin, Q.; Zhang, X.; Zhu, N.; Kusumah, S.; Umemura, K.; Zhao, Z. 2023. Preparation and investigation of an eco-friendly plywood adhesive composed of sucrose and ammonium polyphosphate. *Wood Material Science and Engineering* 18(4): 1202-1211. https://doi.org/10.1080/17480272.2022.2121176

Lu, L.; Chen, B.; Gao, D.; Wang, X. 2024. Push-out test on bolt connectors of H-section steel-laminated bamboo lumber composite structure. *Journal of Forestry Engineering* 9(6): 27-36. https://doi.org/10.13360/j.issn.2096-1359.202401035

Miao, Y.; Pan, S.; Xu, W. 2022. Staple holding strength of furniture frame joints constructed of plywood and solid wood. *Forests* 13. e2006. https://doi.org/10.3390/f13122006

Prekrat, S.; Smardzewski, J. 2010. Effect of glueline shape on strength of mortise and tenon joint. *Drvna Industrija* 61(4): 223-228. https://hrcak.srce.hr/62476

Qi, Y.; Sun, Y.; Zhou, Z.; Huang, Y.; Li, J.; Liu, G. 2023. Response surface optimization based on freeze-thaw cycle pretreatment of poplar wood dyeing effect. *Wood Research* 68(2): 293-305. https://doi.org/10.37763/wr.1336-4561/68.2.293305
Smardzewski, J. 2008. Effect of wood species and glue type on contact stresses in a mortise and tenon joint. *Proceedings of the Institution of Mechanical Engineers, Part C: Journal of Mechanical Engineering Science* 222: 2293-2299. https://doi.org/10.1243/09544062JMES1084
Tang, L.; Guan, H.; Dai, P. 2019. Improved design of three-way mitered joint based on numerical control machining. *Journal of Forestry Engineering* 4(2): 146-151. https://doi.org/10.13360/j.issn.2096-1359.2019.02.023
Tang, L.; Lu, L.; Guan, H. 2022. Modern optimized design and anti-bending property of traditional corner joints. *Journal of Forestry Engineering* 7(4): 166-173. https://doi.org/10.13360/j.issn.2096-1359.202108007
Uysal, M.; Tasdemir, C.; Haviarova, E.; Gazo, R. 2019. Manufacturing feasibility analysis and load carrying capacity of computer numerical control cut joints with interlocking assembly feature. *BioResources* 14(1): 1525-1544. https://doi.org/10.15376/biores.14.1.1525-1544
Wang, Y.; Yan, X. 2024. Preparation of *Toddalia asiatica* (L.) Lam. extract microcapsules and their effect on optical, mechanical and antibacterial performance of waterborne topcoat paint films. *Coatings* 14. e655. https://doi.org/10.3390/coatings14060655
Xiong, X.; Yang, L.; Xu, X.; Fu, S.; Yue, X. 2024. Status of research and application of intelligent manufacturing technology for solid wood furniture in China. *Journal of Forestry Engineering* 9(5): 27-35. https://doi.org/10.13360/j.issn.2096-1359.202312007
Xue, K. 2013. Analysis on the structural performance of traditional Chinese furniture and the design improvement of mortise and tenon joint. PhD Thesis. Nanjing Forestry University
Yu, Y.; Buck, D.; Yang, H.; Du, X.; Song, M.; Wang, J.; Zhu, Z. 2023. Cutting power, temperature, and surface roughness, a multiple target assessment of beech during diamond milling. *Forests* 14. e1163. https://doi.org/10.3390/f14061163
Záborsky, V.; Boruvka, V.; Kašičková, V.; Ruman, D. 2017a. Effect of wood species, adhesive type, and annual ring directions on the stiffness of rail to leg mortise and tenon furniture joints. *BioResources* 12(4): 7016-7031. https://doi.org/10.15376/biores.12.4.7016-7031
Záborsky, V.; Boruvka, V.; Ruman, D.; Gaff, M. 2017b. Effects of geometric parameters of structural elements on joint stiffness. *BioResources* 12(1): 932-946. https://doi.org/10.15376/biores.12.1.932-946
Zou, Y.; Xia, Y.; Yan, X. 2024a. Effects of compound use of two UV coating microcapsules on the physicochemical, optical, mechanical, and self-healing performance of coatings on fiberboard surfaces. *Coatings* 14. e1012. https://doi.org/10.3390/coatings14081012
Zou, Y.; Xia, Y.; Yan, X. 2024b. Effect of UV top coating microcapsules on the coating properties of fiberboard surfaces. *Polymers* 16. e2098. https://doi.org/10.3390/polym16152098
Zhao, Y.; Guan, H.; Zhang, X. 2021. Optimized design of three-way mitered joint structure. *Furniture* 42(5): 35-39. https://doi.org/10.16610/j.cnki.jiaju.2021.06.013

Zheng, Z.; Li, Z.; Guo, S. 2024. Lightweight design of seat based on parametric modeling and 3D printing. *Journal of Forestry Engineering* 9(5): 180-188. https://doi.org/10.13360/j.issn.2096-1359.202310031
Zhou, C.; Zhang, X.; Kaner, J. 2024a. Examining the factors affecting sustained use in smart interactive cabinet design: a comparative analysis using SEM and fsQCA. *Heliyon* 10. e39715. https://doi.org/10.1016/j.heliyon.2024.e39715
Zhou, C.; Yu, R.; Kaner, J. 2024b. Evaluating functional ability in older adults' object retrieval behavior from kitchen furniture using OpenPose and REBA. *Scientific Reports* 14. e25560. https://doi.org/10.1038/s41598-024-75470-6
Zhu, J.; Niu, J. 2022. Green material characteristics applied to office desk furniture. *BioResources* 17(2): 2228-2242. https://doi.org/10.15376/biores.17.2.2228-2242